Poly(L-lactide) Substrates with Tailored Surface Chemistry by Plasma Copolymerisation of Acrylic Monomers

Cristina González García, Llorenç Latorre Ferrus, David Moratal, Manuel Monleón Pradas,* Manuel Salmerón Sánchez*

The wettability of PLLA substrates was modified by plasma copolymerising on its surface thin films based on EA and HEA. The composition of the reactive gas inside the plasma chamber was that of the corresponding liquid mixture of the comonomers. The surface of the substrates was investigated by AFM, which showed that the plasma film was ≈100 nm thick. The WCA decreases monotonically with decreasing HEA content in the mixture. The fraction of hydroxyl groups has been calculated from XPS. The local mechanical properties of the plasma-polymerised surfaces were estimated by nanoindentation experiments performed using the AFM tip, which turns out to be a method sensitive to the composition of the copolymerised plasma film on the PLLA surface.

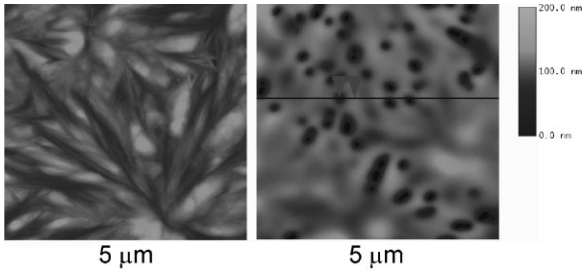

Introduction

Poly(L-lactic acid), PLLA, is a biocompatible and biodegradable polymer widely used in biomedical applications.[1–4] PLLA is a promising material in biomedicine since it degrades through hydrolytic scission of the ester groups into lactic acid. The kinetics of bioresorption depends on the crystallinity and the semi-crystalline morphology and, in general, it is faster in the amourphous domains (inter/intra spherulitic) than within the crystallites.[5,6] PLLA is hydrophobic in nature and it is convenient for some applications to increase the surface wettability keeping its bulk properties unaffected. Surface treatments on PLA include NaOH hydrolysis,[7] aminolysis by poly(allylamine hydrochloride) at high pH and subsequent electrostatic self-assembly of poly(sodium styrenesulfonate),[8] grafting poly(hydroxyethyl methacrylate) or poly(methacrylic acid) via photooxidisation and subsequent UV-induced polymerisation,[9] surface modification with chitosan, via entrapment and coupling by using 1-ethyl-3-(3-dimethylaminopropyl)carbodiimide and *N*-hydroxysuccinimide,[10] and several processes which involve plasma treatments at some step.[11–15]

Even if plasma polymerisation on the surface of a material is a versatile route to change the outer chemistry of the system,[16–19] the introduction of two precursors into the plasma chamber, so-called plasma copolymerisation, strengthens the possibilities of the technique by allowing one to deposit different chemical functionalities, at different proportions, to tailor the physico-chemical properties of the surface more accurately. By this

C. González García, L. Latorre Ferrus, D. Moratal, M. Monleón Pradas, M. Salmerón Sánchez
Center for Biomaterials and Tissue Engineering, Universidad Politécnica de Valencia, 46022 Valencia, Spain
Fax: +34 9638 7727; E-mail: masalsan@fis.upv.es
M. Monleón Pradas, M. Salmerón Sánchez
Regenerative Medicine Unit. Centro de Investigación Príncipe Felipe, Autopista del Saler 16, 46013 Valencia, Spain
C. González García, M. Monleón Pradas, M. Salmerón Sánchez
Networking Research Centre on Bioengineering, Biomaterials and Nanomedicine (CIBER-BBN), Valencia, Spain

Plasma Process. Polym. **2009**, *6*, 190–198

DOI: 10.1002/ppap.200800112

approach, a relatively small number of systems have been prepared to develop (bio)technologically required surface properties, which include the surface modification of intraocular lenses,[20] and controlling the surface chemistry at the cell-material interaction with bone marrow stromal cells and keratinocytes.[21,22] There is a set of fundamental questions related to plasma copolymerisation which remain to be solved. The relationship between the functional group concentration in plasma copolymerised substrates and the feed gas composition does not seem to have a unique trend and linear,[23] as well as non-linear[24–26] correlations have been reported depending on the chemical nature of the feed gas mixture.[26] Interactions between the reacting monomers in the gas chamber gives rise in some cases to the formation of new species that were not present in coatings produced from the individual parents monomers.[27]

This work presents the plasma copolymerisation of ethyl acrylate, EA, and hydroxyethyl acrylate, HEA, which have a vinyl backbone chain with the side groups $-COOCH_2CH_3$ and $-COOCH_2CH_2OH$, respectively, onto PLLA substrates aiming to tailor the surface wettability of PLA. The feed gas mixture is obtained by conducting a liquid mixture of both comonomers into the chamber, rather than by introducing the two different monomer flows at different mass ratios into the plasma chamber. The physico-chemical properties of the resulting surfaces are investigated. The water contact angle (WCA) characterises the wettability of the substrate. The chemical composition of the surface is quantified by means of deconvolution of the X-ray photoelectron spectroscopy (XPS) experiments for C1s and O1s. The topology of the surfaces is investigated by atomic force microscopy (AFM), and the local mechanical properties by indentation experiments at the nanoscale by making use of the AFM tip.

Experimental Part

Materials

PLLA was synthesised by classical polycondensation procedures. The polymerisation reactions were carried out as described elsewhere.[28] Briefly, a glass polymerisation reactor equipped with a nitrogen flow through inlet and a vacuum connection was placed in a temperature-controlled bath containing silicone oil. Polymerisation was performed for 12–48 h in a nitrogen atmosphere within a temperature range of 100–150 °C. To remove residual monomers, chloroform and methanol were used as solvent and precipitant, respectively. The characteristic molar masses of the polymer, $\overline{M}_n$ and $\overline{M}_w$, were 58 000 and 132 000 $g \cdot mol^{-1}$, respectively, as evaluated by gel permeation chromatography (Shimadzu, LC 10A, Japan) using polystyrenes as standards and chloroform as solvent.

Samples used for surface modification were spin-cast (Brewer Science, Rolla, USA) from a 2 wt.-% solution in chloroform on circular microscopy slides ($\phi = 12$ mm) by spinning at 2 000 rpm for 30 s. The thickness of the PLLA layer was around 400 nm, estimated from subsequent AFM images.

Monomers of ethyl acrylate (EA, Aldrich, 99% pure) and hydroxyethyl acrylate (HEA, Aldrich 96% pure) were employed without further purification. Mixtures of the comonomers with different mass ratios were prepared and injected into the plasma chamber by using a pressurised device specially designed for us by Plasma Electronic GmbH (Germany). Five monomer feed compositions were chosen, given by the fraction of HEA in the initial mixture of 1, 0.7, 0.5, 0.3, and 0 (hereafter $-OH_x$, will refer to the sample with fraction x of HEA in the feed mixture). The plasma discharge was performed in a Piccolo apparatus (Plasma Electronic), which has a stainless steel vacuum chamber with a volume of 45 L. Plasma was generated using a 2.45 GHz Gigatron® device for low-pressure plasmas. The liquid mixture of monomers was introduced in the pressurised device which was connected to an argon line. Figure 1 sketches the experimental setup. The process started with the evacuation of the air present inside the chamber until a base pressure of 50 Pa was achieved. The composition of the reactive gas inside the plasma chamber was that of the corresponding monomer mixture, since the liquid mixture is conducted from the pressure tank to the chamber by the argon current until it is vapourised into the chamber at 160 sccm. After 15 s of homogenisation, to assure full distribution of the process gas in the vacuum chamber, as well as that all traces of air or previous process gas are removed from the chamber, the plasma was generated at 50 Pa and 360 W for 300 s giving rise to the copolymerisation of the feeding mixture. Afterwards, samples were kept in a vacuum desiccator to remove non-grafted chains before characterisation.

Surface Properties

WCAs were measured (using a Dataphysics OCA) for the different substrates before (PLLA) and after plasma copolymerisation at different feed ratios. The stability of the measurements was checked up to 30 d after the surface treatment.

XPS experiments were performed in a PHI 5500 Multitechnique System (from Physical Electronics) with a monochromatic X-ray source (Aluminium K_α line of 1 486.6 eV energy and 350 W), placed perpendicularly to the analyser axis and calibrated using the $3d_{5/2}$ line of Ag with a full width at half maximum (FWHM) of 0.8 eV.

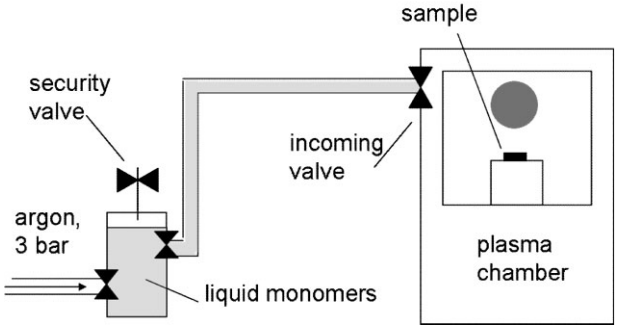

Figure 1. Sketch of the experimental setup. The liquid mixture of co-monomers is entrained by the argon flow from the pressurised device to the plasma chamber, where it is vapourised.

The analysed area was a circle of 0.8 mm diametre, and the selected resolution for the spectra was 187.5 eV of pass energy and 0.8 eV · step^{-1} for the general spectra, and 23.5 eV of pass energy and 0.1 eV · step^{-1} for the spectra of the different elements. All measurements were made in an ultra high vacuum (UHV) chamber pressure between 5×10^{-9} and 2×10^{-8} Torr. XPS elemental sensitivity factors according to the MULTIPAK program for PHI instruments were used. Charge compensation was performed experimentally by using a low energy electron gun.

An automatic XPS signal fitting software has been developed under MATLAB v7.2 (The MathWorks, Inc, Natick, MA, USA) environment to deconvolute the experimental spectra. The analysis performs lineshape fitting in the energy axis and enables estimation of energies, intensities and linewidths of individual peaks. An iterative method based on the Levenberg-Marquardt non-linear least squares optimisation algorithm is used. The program uses a Gaussian/Lorentzian lineshape. The fitting software makes use of an independent Voigt function per peak (which in our case means four Voigt functions to fit the C 1s spectra and three Voigt functions to fit the O 1s peaks). Each Voigt function consists of four parametres (intensity, FWHM associated to the Lorentzian function, the standard deviation associated to the Gaussian function and the binding energy at which the Voigt function is centred). During the fitting procedure, the intensity has been constrained to be positive and the rest of parametres are constrained within a defined range, typically to be lower than 0.5 both for the FWHM of the Lorentzian function and the standard deviation of the Gauss function.

Atomic Force Microscopy and Nanoindentation

AFM was performed in a NanoScope III from Digital Instruments (Santa Barbara, CA) operating in the tapping mode in air; Nanoscope 5.30r2 software version was used. Si-cantilevers from Veeco (Manchester, UK) were used with force constant of 2.8 N · m^{-1} and resonance frequency of 75 kHz. The phase signal was set to zero at a frequency 5–10% lower than the resonance one. Drive amplitude was 200 mV and the amplitude set point A_{sp} was 1.4 V. The ratio between the amplitude set point and the free amplitude A_{sp}/A_0 was kept equal to 0.7.

Indentation experiments were conducted with a Veeco square pyramidal tip OTR8 with a spring constant 0.57 N · m^{-1} (datum supplied by the manufacturer) and tip half angle 35°. Calibration of the tip sensitivity was performed in the same conditions as the experiments with a flat surface sample made of the same material than the tip, and was calculated to be 5.721 nm · V^{-1} after at least 10 repetitions. Sensitivity of the tip was used to correct the deflection of the tip due to the vertical movement of the sample without penetration. All experiments were performed with the instrument mounted on a vibration isolation system.

Results and Discussion

Figure 2 shows the chemical structure corresponding to the homopolymers poly(ethyl acrylate) and poly(hydroxyethyl acrylate).

Figure 3 shows the substrate wettability as obtained from water contact angle measurements on the different

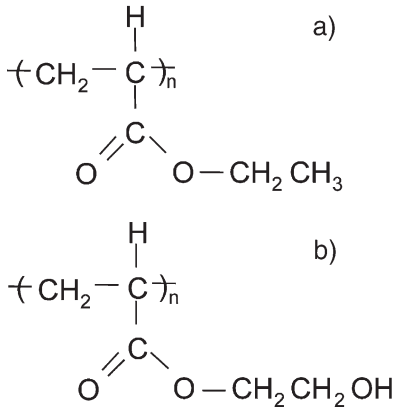

Figure 2. Chemical structure of the homopolymers corresponding to the monomers injected in the plasma chamber. a) poly(ethyl acrylate), b) poly(hydroxyethyl acrylate).

substrates after plasma copolymerisation from initial comonomer mixtures (EA and HEA), and the plane PLLA. Water contact angle increases monotonically from 45° to 80° as the fraction of HEA in the feed solution decreases. The only difference between both comonomers is in the side groups $-COOCH_2CH_3$ and $-COOCH_2CH_2OH$ for EA and HEA respectively, which explains the hydrophilic character of HEA, due to the presence of hydroxyl groups, and the

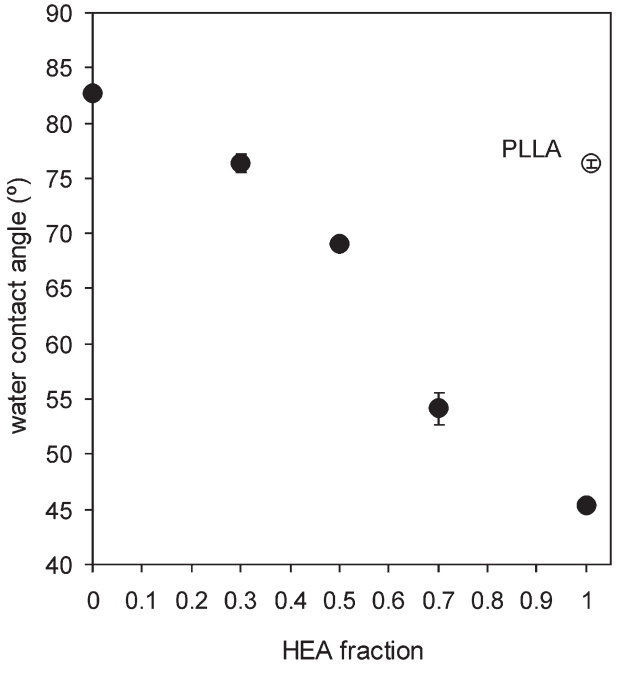

Figure 3. Water contact angles of the plasma copolymerised layer deposited on the PLLA substrate as a function of the fraction of HEA comonomer in the EA/HEA feeding mixture. The open circle represents the result for the underlying PLLA substrate. The standard deviation of five independent measurements is included. When not visible, is lower than the size of the symbol.

DOI: 10.1002/ppap.200800112

comparatively more hydrophobic nature of EA. Surface wettability is a very sensitive parametre to surface chemistry,[29] and its monotonic change suggests that the plasma polymerised film contains increasing fractions of hydrophilic units as the fraction of this co-monomer in the feed mixture increases. Nevertheless, one cannot discard fragmentation of the original monomers, HEA and EA units, in the plasma (even at this fairly low power), which will result in the formation of new functional groups that were not present in the precursors.

Further insight into the substrate surface chemistry can be gained from XPS measurements. Figure 4a and b show the experimental high resolution scans in the oxygen region (O1s) of the deposited films polymerised from different feed mixtures. The peaks of the spectra become higher and wider as the amount of HEA in the feed mixture increases (Figure 4b). The experimental peaks can be deconvoluted by means of Voigt functions.[30] HEA and EA units share two oxygen moieties, C=O* oxygen (≈ 532.3 eV) and the OC–O* oxygen (≈ 533.8 eV).[31] The asterisk denotes the atom with which the binding energy is associated. However, only the HEA units contain the O*–H oxygen (≈ 533.1 eV).[31] Figure 4c shows representative curves for one of the copolymers after the fitting process. The fraction of HEA units in the copolymer, i.e. the concentration of OH groups in the surface, has therefore been characterised by considering the area under the O*–H component curve of the deconvoluted XPS spectra. This area is found to increase as the fraction of HEA in the feeding mixture increases (Table 2).

The fraction of HEA in the surface can be independently estimated from XPS spectra in the carbon (C1s) region. Figure 5a and b show the experimental curves for the different plasma copolymerised systems. The shape of the individual spectra is qualitatively the same but there is a shoulder at the higher energy side which increases monotonically as the amount of HEA in the feeding mixture does. HEA and EA share four carbon moieties: C–H_2 (≈ 285 eV), O–C=O (≈ 289 eV), C–O (≈ 287 eV) and C–COOR (≈ 285.7 eV); only the HEA units contain the C–OH carbon (≈ 286 eV).[31] Figure 5c shows a representative deconvolution for one experimental spectrum. As for the case of the XPS oxygen spectra, the fraction of HEA units in the copolymer can then be characterised by considering the area under the C–OH component curve of the deconvoluted C1s spectra, which is found to increase as the fraction of HEA in the feed mixture increases (Table 1).

Figure 6 shows quantitative calculations for the XPS O/C atomic ratios from the experimental curves. The oxygen surface concentration in the films increases as the amount of HEA in the feeding mixture does, Figure 6a. The theoretical O/C ratio for the homopolymers based on the structure of pure EA and HEA are 0.4 and 0.6 respectively, (Figure 2), in agreement with those obtained experimentally (0.37 and 0.8 respectively). The difference in the case of HEA might be related to the fragmentation of the monomers in the plasma chamber giving rise to the formation of new functional groups that have not been taken into account in the analysis. The oxygen surface concentration does not depend linearly on the amount of initial HEA present in the feed mixture. Moreover, the O/C atomic ratio in the surface of the copolymers is lower than expected from the linear combination of the corresponding homopolymers. Since the only difference between HEA and EA co-monomers lies in the presence of the C–OH group in the last one, the relative areas of the peak associated to the carbon (C1s) and oxygen (O1s) in the deconvoluted spectra (Table 1 and 2) allows one to calculate the surface concentration of hydroxyl groups. Figure 6b shows the ratio between the area associated to the C–OH carbon in the different copolymers to that obtained for the PHEA homopolymer after the corresponding deconvolution procedure of the XPS spectra.

The observed trend can be understood in terms of classical copolymerisation theory even though the plasma polymerisation mechanism is not expected to be a pure free radical polymerisation mechanism.[32] The relationship between monomer structure and reactivity depends

Table 1. Results of the deconvolution procedure of the experimental XPS spectra for the plasma copolymerised films in the C1s region. Correction for charging was taken into account by setting the CH_2 peak to 285.0 eV.

HEA	C*OH		C*OO		COC*		CH_2		C*–COOR	
	BE	Area	BE	Area	BE	Area	BE	Area	BE	Area
%	eV	%	eV	%	eV	%	eV	%	eV	%
100	286.0	15	289.2	13	287.2	11	285.0	47	285.8	14
70	285.9	10	289.2	10	287.3	12	285.0	52	285.8	15
50	285.8	6	288.8	12	287.0	11	285.0	56	285.9	16
30	285.8	3	288.9	13	287.3	12	285.0	57	285.7	14
0	–	–	288.8	11	287.4	15	285.0	56	285.9	17

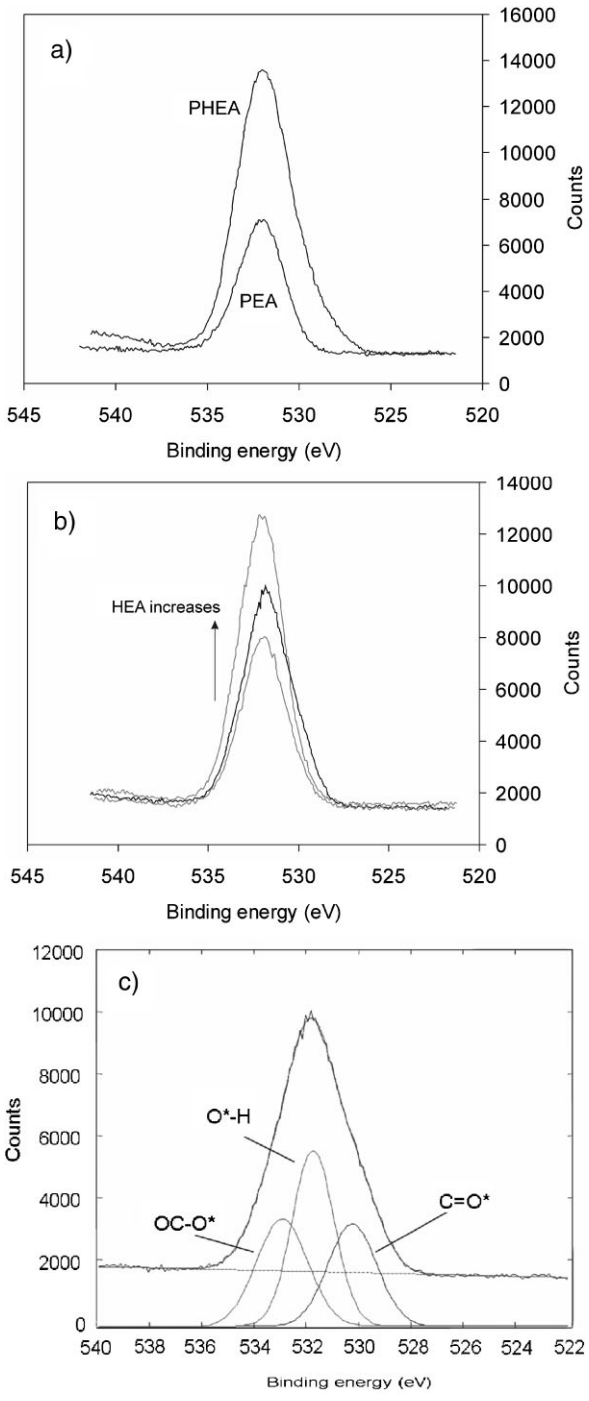

Figure 4. XPS spectra in the O1s regions for the polymerised a) homopolymers and b) copolymers. HEA fraction in b) includes 0.3, 0.5 and 0.7. c) Characteristic deconvolution for the O1s XPS spectrum (the curve shown corresponds to the 0.5 HEA system).

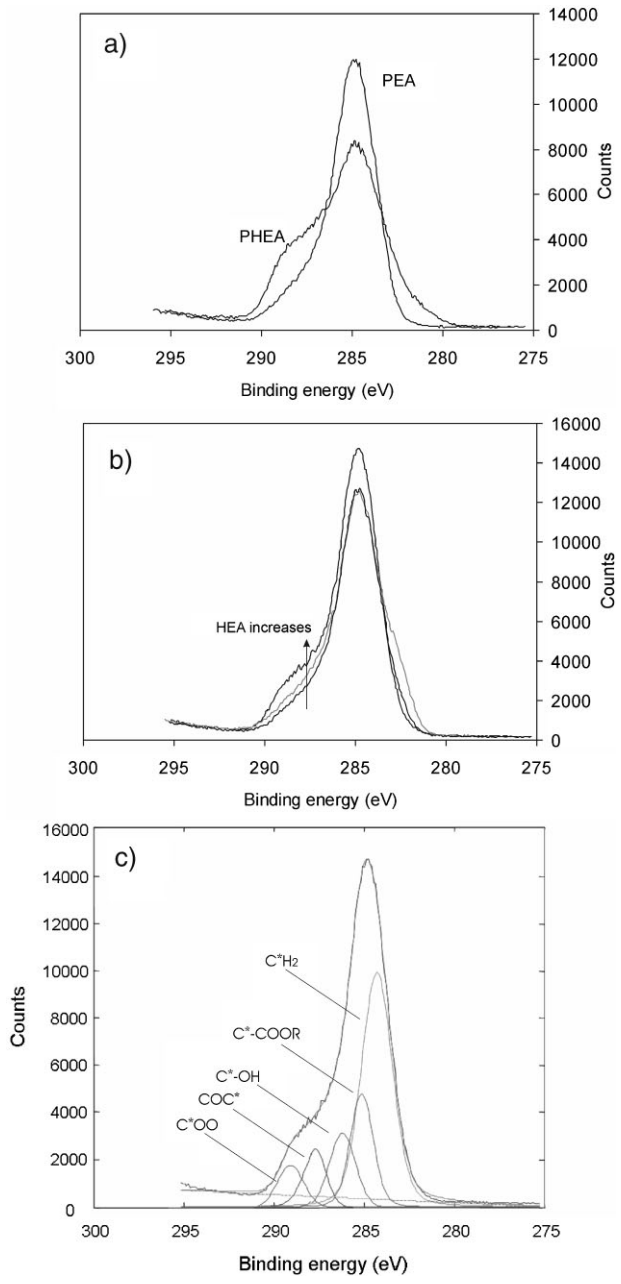

Figure 5. XPS spectra in the C1s regions for the polymerised a) homopolymers and b) copolymers. HEA fraction in b) includes 0.3, 0.5 and 0.7. c) Characteristic deconvolution for the C1s XPS spectrum (the curve shown corresponds to the 0.7 HEA system).

on the resonance degree and polar factors. The Q-e scheme proposed by Alfrey and Price allows one to predict the reactivity ratios.[33] The values for EA and HEA monomers are $Q_{EA} = 0.42$, $e_{EA} = 0.22$, $Q_{HEA} = 0.84$, $e_{HEA} = 0.68$,[34] which determine the reactivity ratios to be 0.68 and 1.18. The Q-e prediction overestimates the reactivity ratios obtained experimentally by, e.g., the method proposed by Fineman-Ross[35]; 0.5 and 0.97 for EA and HEA respectively.[34] Copolymerisation theory allows estimating, via the terminal model, the composition of the copolymer chain once the polymerisation process is finished.[32,36] The monomer i molar fraction F_i in the copolymer in terms of the monomer molar fraction in the reaction mixture f_i and

Plasma Process. Polym. **2009**, *6*, 190–198

DOI: 10.1002/ppap.200800112

Table 2. Results of the deconvolution procedure of the experimental XPS spectra for the plasma copolymerised films in the O1s region. Correction for charging was taken into account by setting the CH_2 peak to 285.0 eV.

HEA	C=O*		OC–O*		O*–H	
	BE	Area	BE	Area	BE	Area
%	eV	%	eV	%	eV	%
100	531.2	35	533.8	28	532.4	37
70	531.7	39	533.7	32	532.5	29
50	531.1	41	533.6	37	532.5	22
30	531.2	41	533.4	47	532.4	12
0	531.1	45	533.1	55	–	–

the reactivity ratios r_i turns out to be:

$$\frac{F_1}{F_2} = \frac{f_1(f_1 r_1 + f_2)}{f_2(f_2 r_2 + f_1)} \quad (1)$$

The different reactivity ratios have an immediate consequence. HEA monomers have a higher tendency to react with HEA monomers than with the EA ones. On the other hand, the lower EA reactivity ratio means that this monomer has a higher affinity towards HEA monomers than towards the EA ones. The composition predicted by the terminal model, Equation (1), is drawn as a continuous line in Figure 6b. The theoretical prediction lies above the straight line that gives the random composition of the copolymer chain (that is, the final copolymer keeping the same proportion of the two components present in the original feed mixture). Area calculations from the deconvoluted XPS spectra (dots in Figure 6b) do not follow the general trend suggested by the terminal model, i.e. the slight preference for homopolymerisation of HEA is not found. Moreover, copolymer chain compositions as obtained from XPS suggest higher fraction of EA units (that is, lower surface concentration of OH groups) in the plasma polymerised systems. Nevertheless, one cannot discard fragmentation of the original monomers, HEA and EA units, in the plasma (even at this fairly low power) which will result in the formation of new functional groups that were not present in the precursors. In this case, the role of the chemical reactivity would be less important.

Figure 7 shows AFM images of the PLLA substrates before and after plasma polymerisation. The surface of the spin cast PLLA film is so smooth that the plasma layer coated on it cannot be directly observed in Figure 7b. Exploiting the semicrystalline character of PLLA, we have isothermally crystallised PLLA substrate at 110 °C for 2 h after a nucleation treatment at 75 °C to get small

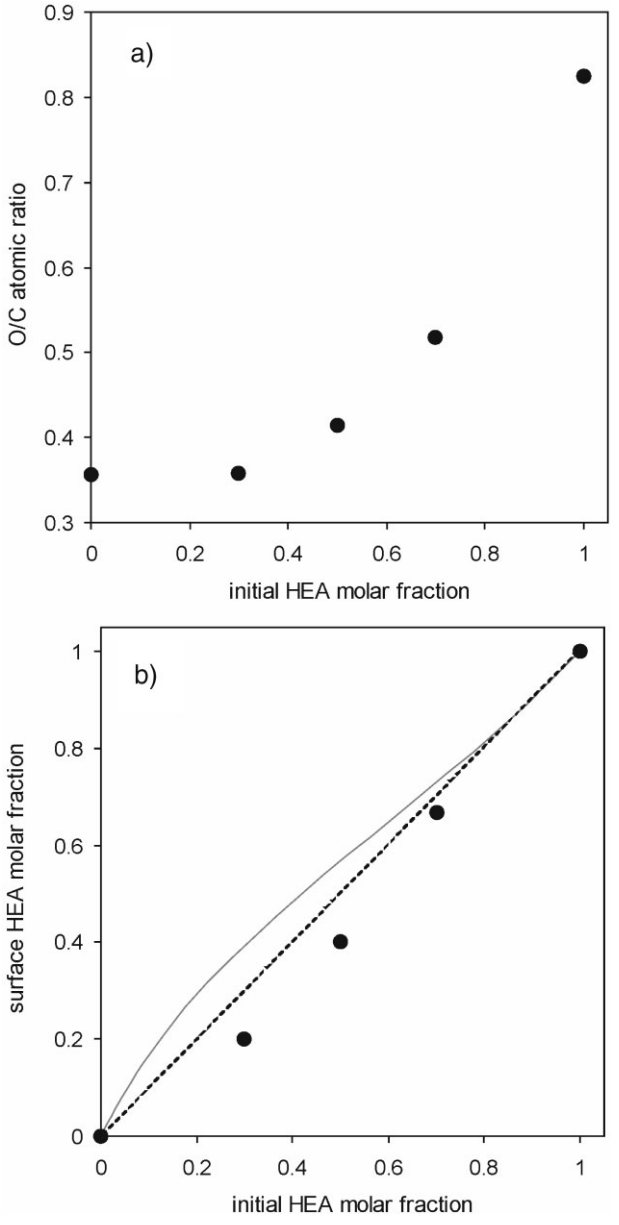

Figure 6. Quantification of the XPS spectra: a) XPS O/C atomic ratio vs. the concentration of HEA in the feeding mixture. b) Fraction of HEA in the copolymerised systems calculated from the ratio of areas associated to the C–OH peak in the copolymers and the PHEA homopolymer. The continuous line is the prediction of the terminal model (Equation 1 in the text).

spherulites (≈5 μm in diametre) seeking to increase the surface roughness before plasma polymerisation.[37] Figure 7c and d show the original PLLA spherulites (the substrate) and the plasma deposited layer on them (the coatings), respectively. Figure 7d shows some defects in the plasma layer (that were not present in the original PLA substrate), which can be employed to estimate the thickness of the coating by analysing a cross section through one such defect. This is done in Figure 7e, which

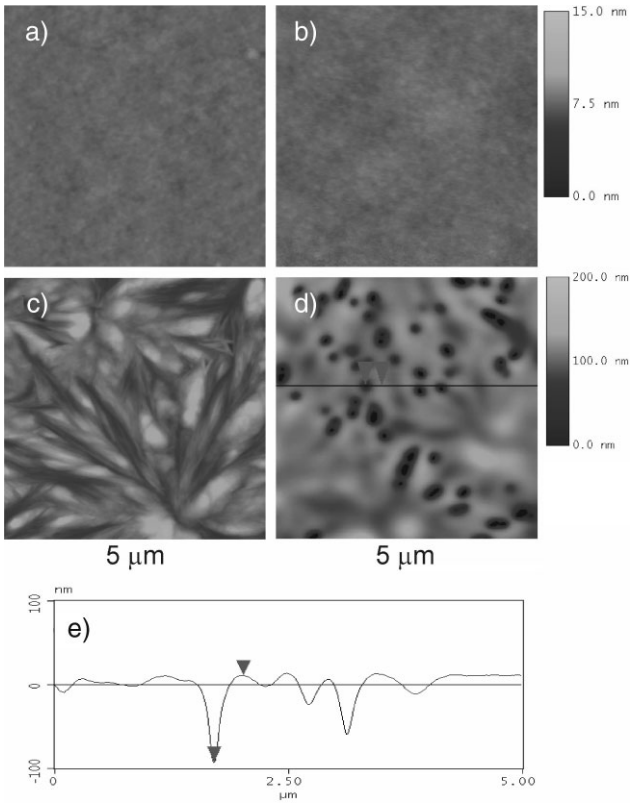

Figure 7. AFM images (height magnitude) of the substrates. a) plane PLLA substrate before plasma treatment. b) PLLA substrate after plasma polymerisation of HEA on its surface. c) Semicrystalline PLLA substrate before plasma treatment showing in detail a small spherulite grown from the melt at 110 °C for 2 h after nucleating at 75 °C for 6 h. d) Semicrystalline PLLA substrate after plasma polymerisation of HEA on its surface. The black small-circles are defects in the deposited film. e) Cross-section of the plasma polymerised coating along the black line in d). The distance between the two arrows gives an approximation of the film thickness.

shows that the thickness of the plasma polymer layer is below 100 nm.

Additional information on the nature of the plasma polymerised coating can be gained from nanoindentation experiments. AFM can be used as a nanoindenter to perform force-volume probes without further specialised depth-sensing instruments.[38] In force-volume assessments, a rigid sharp tip interacts with a surface while applied force and penetration depth are recorded. An array of indentations is normally performed along the target surface, and for each indentation measurement a force/displacement curve is obtained. Those plots normally collect the loading and unloading cycles, which must coincide if material's behaviour is purely elastic. On the contrary, hysteresis loops appear when viscoelastic materials are studied.[38] The result of one of these experiments is shown in Figure 8, where the force is

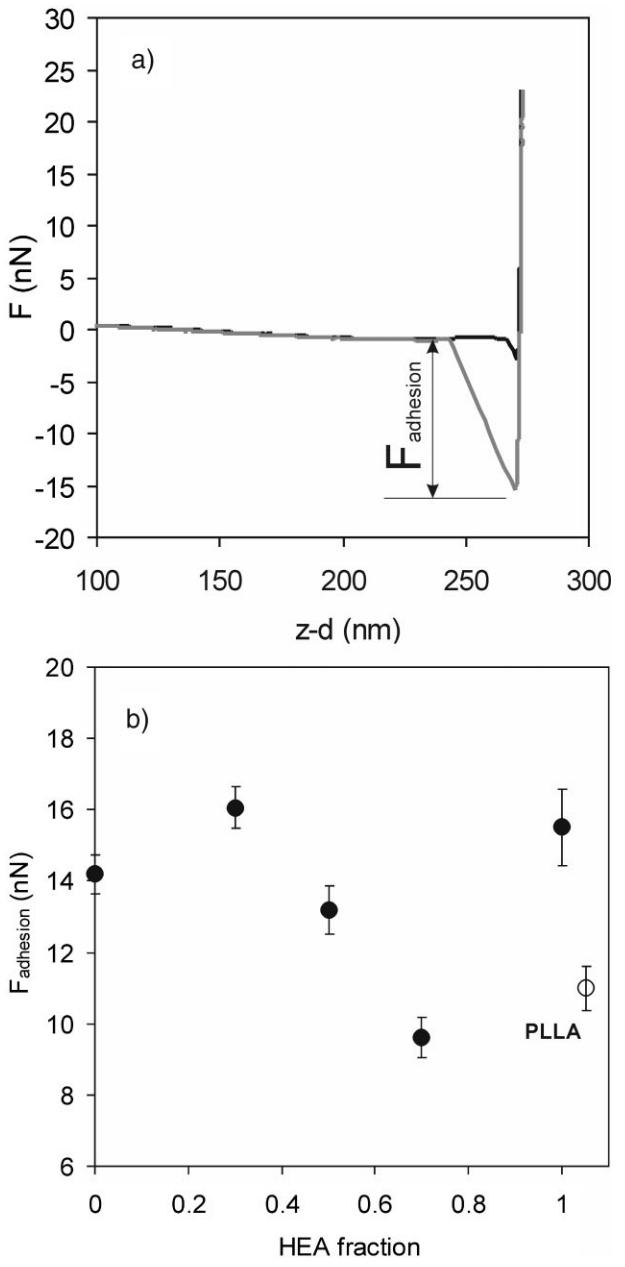

Figure 8. a) Measured force in an indentation AFM experiment against the difference between the *z* displacement of the sample and the cantilever deflection *d*. The black line represents the indentation scan and the thin one the retraction one. The adhesion force has been calculated as indicated in the graph. b) Adhesion forces between the tip and the sample during the indentation experiments as a function of the HEA fraction in the feeding mixture. The error bar represents the standard deviation of 750 experimental curves.

represented against the difference between the displacement of the sample in the vertical axis, *z*, and the cantilever deflection, *d*. The variable $z - d$ is the relative displacement between the tip and the polymer surface. At low values of

Plasma Process. Polym. **2009**, *6*, 190–198

DOI: 10.1002/ppap.200800112

$z - d$, there is no contact between the tip and the surface (both the deflection of the cantilever and the measured force are near zero). The black line (Figure 8a) is obtained during indentation scan, while the grey one corresponds to the retracting scan. The negative values of the force (adhesion force between the tip and the surface due to van der Waals long-range interactions) are produced close to the contact point,[39] which can be determined as shown in Figure 8 (i.e. it is the intersection point between the experimental curve and the horizontal reference assumed in absence of contact).[40] For greater values of relative displacement $z - d$, short-range repulsive interactions take place between sample and tip as well as the indentation of the material, which overcome the previous attraction forces making the force F to increase.

The adhesion force between the tip and the substrate is shown in Figure 8b. Both plasma polymerised PHEA and PEA (HEA fraction equal to 1 and 0, respectively, in the graph) show similar adhesion forces, which are higher than those for the underlying PLLA substrate. This is a direct physical proof for the presence of the plasma polymerised coating. Nevertheless, the adhesion force is not constant for the different substrates, but its value varies in a non linear way between those of the homopolymers and that of the PLLA substrate. The presence of small amounts of EA in the system (lower that 0.3) led to the reduction in the adhesion force from 15.5 to 9.6 nN. As the amount of EA in the system increases (i.e. HEA decreases), the adhesion force increases monotonically up to the PHEA homopolymer value.

Indentation experiments were performed on all the samples at sets of 50 points located on a straight line and separated 10 nm from each other, covering a distance of 500 nm. Five parallel lines separated 20 nm from each other were scanned. Experiments were performed in triplicate on different samples. The penetration of tip inside the sample was kept below 30 nm, to assure that only the response of the plasma polymerised coating was considered. Our results show that the adhesion force between the AFM tip and the substrate is sensitive to the chemical composition changes of the surface. The non-linear dependence between the adhesion force and the copolymer composition, suggests the synergistic character of the EA and HEA molecules distributed along the copolymer chain regarding the adhesion force.

Conclusion

The surface properties of a PLLA substrate have been modified by plasma copolymerisation of acrylic monomers based on ethyl acrylate and hydroxyethyl acrylate. The wettability of the treated substrates was modified in a controlled way as reflected by the values of water contact angles increasing monotonically from 45 to 83° as the fraction of HEA in the copolymerised layer decreases. The composition of the plasma copolymerised system was assessed by deconvolution of the XPS C1s and O1s spectra and compared with the prediction of the classical copolymerisation theory, i.e. the terminal model, based on the composition of the feed mixture. The plasma copolymerised layer on the surface of the PLLA substrate presents a lower mass fraction of HEA units than the corresponding feed mixture of comonomers, in contrast with the classical terminal model for copolymerisation.

The thickness of the deposited plasma film was estimated to be approximately 100 nm from AFM images. Nanoindentation experiments allow one to calculate the adhesion force between the AFM tip and the sample, which results to be a physical quantity very sensitive to chemical composition differences between the substrate and the distribution of the comonomer units within the plasma polymerised chain.

Acknowledgements: AFM analyses were performed under the technical guidance of the Microscopy Service at the *Universidad Politécnica de Valencia*, whose advice is greatly appreciated. Authors acknowledge the reviewer's comments and suggestions which improved the quality of the manuscript. The support of the *Spanish Ministry of Science* through project No. MAT2006-08120 (including the *FEDER* financial support) is kindly acknowledged.

Received: August 7, 2008; Revised: November 7, 2008; Accepted: November 14, 2008; DOI: 10.1002/ppap.200800112

Keywords: atomic force microscopy (AFM); biomaterials; plasma polymerization; surface modification; XPS

[1] A. Södegard, M. Stolt, *Prog. Polym. Sci.* **2002**, *27*, 1123.
[2] R. C. Thomson, M. C. Wake, M. J. Yaszemski, A. G. Mikos, *Adv. Polym. Sci.* **1995**, *122*, 245.
[3] H. D. Kim, E. H. Bae, I. C. Kwon, R. R. Pal, J. D. Nam, D. S. Lee, *Biomaterials* **2004**, *25*, 2319.
[4] Z. Ma, C. Gao, Y. Gong, J. Shen, *Biomaterials* **2005**, *26*, 1253.
[5] M. Reeve, S. McCarthy, M. Downey, R. Gross, *Macromolecules* **1994**, *27*, 825.
[6] R. MacDonald, S. McCarthy, R. Gross, *Macromolecules* **1996**, *29*, 7356.
[7] Y.-Q. Wang, J.-Y. Cai, *Curr. Appl. Phys.* **2007**, *7S1*, e108.
[8] Y. Lin, L. Wang, P. Zhang, X. Wang, X. Chen, X. Jing, Z. Su, *Acta Biomater.* **2006**, 2155.
[9] Z. Ma, C. Gao, J. Ji, J. Shen, *Eur. Polym. J.* **2002**, *38*, 2279.
[10] Y. L. Cui, A. D. Qi, W. G. Liu, X. H. Wang, H. Wang, D. M. Ma, K. D. Yao, *Biomaterials* **2003**, *24*, 3859.
[11] Z. Ding, J. Chen, S. Gao, J. Chang, J. Zhang, E. T. Kang, *Biomaterials* **2004**, *25*, 1059.
[12] Y. L. Cui, X. Jou, A. D. Qi, X. H. Wang, H. Wang, K. Y. Cai, Y. Yin, K. De Cao, *J. Biomed. Mater. Res.* **2003**, *66*, 770.
[13] H. Suh, Y. S. Hwang, J. E. Lee, C. D. Han, J. C. Park, *Biomaterials* **2001**, *22*, 3545.
[14] M. T. Khorasani, H. Mirzadeh, S. Irani, *Radiat. Phys. Chem.* **2008**, *77*, 280.

[15] M. Nakagawa, F. Teraoka, S. Fujimoto, Y. Yamada, H. Kibayashi, J. Takahashi, *J. Biomed. Mater. Res.* **2006**, *77A*, 112.
[16] R. Förch, Z. Zhang, W. Knoll, *Plasma Process. Polym.* **2005**, *2*, 351.
[17] K. Suzuki, A. Sawabe, H. Yasuda, T. Inuzuka, *Appl. Phys. Lett.* **1987**, *2*, 263.
[18] B. W. Muir, H. Thissen, G. P. Simon, P. J. Murphy, H. J. Griesser, *Thin Solid Films* **2006**, *500*, 34.
[19] A. Serrano Aroca, M. Monleón Pradas, J. L. Gómez Ribelles, *Polymer* **2007**, *48*, 2071.
[20] T. S. Suh, C. K. Joo, Y. C. Kim, M. S. Lee, H. L. Lee, B. Y. Choe, H. J. Chun, *J. Appl. Polym. Sci.* **2002**, *85*, 2361.
[21] R. Daw, T. O'Leary, J. Kelly, R. D. Short, M. Cambray-Daekin, A. J. Devlin, I. M. Brook, A. Scutt, S. Kothari, *Plasmas Polym.* **1999**, *3*, 113.
[22] R. M. France, R. D. Short, E. Duval, F. R. Jones, *Chem. Mater.* **1998**, *10*, 1176.
[23] J. Friedrich, G. Kühn, R. Mix, W. Unger, *Plasma Process. Polym.* **2004**, *1*, 28.
[24] M. R. Alexander, T. M. Duc, *Polymer* **1999**, *40*, 5479.
[25] S. Swaral, U. Oran, A. Lippitz, W. E. S. Unger, *Plasma. Process. Polym.* **2007**, *4*, 376.
[26] S. Swaraj, U. Oran, A. Lippitz, W. E. S. Unger, *Plasma Process. Polym.* **2008**, *5*, 92.
[27] A. Beck, J. D. Whittle, N. A. Bullet, P. Eves, S. M. Neil, S. L. McArthur, A. Shard, *Plasma Process. Polym.* **2005**, *2*, 641.
[28] H. Yavuz, C. Babac, K. Tuzlakoglu, E. Piskin, *Polym. Degrad. Stab.* **2002**, *75*, 431.
[29] A. W. Adamson, "*Physical Chemistry of Surfaces*", John Wiley & Sons, New York 1990.
[30] N. Fairley, "XPS lineshapes and curvefitting", Chapter 15 in: *Surface analysis by Auger and X-ray photoelectron spectroscopy*, E. Briggs, H. Grant, Eds., SurfaceSpectra, IMPublications, Townbridge 2003.
[31] G. Beamson, D. Briggs, "*High Resolution XPS of Organic Polymers: the Scienta ESCA3000 Database*", Wiley, Chichester 1992.
[32] F. R. Mayo, F. M. Lewis, *J. Am. Chem. Soc.* **1944**, *66*, 1594.
[33] T. Alfrey, C. C. Price, *J. Polym. Sci.* **1947**, *2*, 101.
[34] J. Brandrup, E. H. Immergut, in: *Polymer Handbook*, 3rd Ed., *Ch. II*, John Wiley & Sons, New York 1989.
[35] M. Fineman, S. D. Ross, *J. Polym. Sci.* **1950**, *5*, 259.
[36] T. Alfrey, G. Goldfinger, *J. Chem. Phys.* **1944**, *12*, 205.
[37] F. Hernández Sánchez, J. Molina Mateo, J. Romero Colomer, M. Salmerón Sánchez, J. L. Gómez Ribelles, J. F. Mano, *Biomacromolecules* **2005**, *6*, 3283.
[38] J. R. Withers, D. E. Aston, *Adv. Colloid Interface Sci.* **2006**, *120*, 57.
[39] J. Drelich, Z. Xu, J. Masliyah, *Langmuir* **2006**, *22*, 8850.

DOI: 10.1002/ppap.200800112